ELSEVIER

Journal of Power Sources 92 (2001) 35–39

JOURNAL OF POWER SOURCES

www.elsevier.com/locate/jpowsour

Preparation and electrochemical/thermal properties of $LiNi_{0.74}Co_{0.26}O_2$ cathode material

Jaephil Cho[a,*], Byungwoo Park[b]

[a]*Energy Lab, Samsung SDI Co. Ltd., Chungchongnam-Do, Chonan City 330-300, South Korea*
[b]*School of Materials Science and Engineering, Seoul National University, Seoul, South Korea*

Received 17 March 2000; accepted 5 May 2000

Abstract

Electrochemical and thermal properties of $LiNi_{0.74}Co_{0.26}O_2$ cathode material with 5, 13 and 25 μm-sized particles have been studied by using a coin-type half-cell Li/$LiNi_{0.74}Co_{0.26}O_2$. The specific capacity of the material ranges from 205 to 210 mA h g^{-1}, depending on the particle size or the Brunauer, Emmett and Teller (BET) surface area. Among the particle sizes, the cathode with a particle size of 13 μm shows the highest specific capacity. Even though the material with a particle size of 5 μm exhibits the smallest capacity value of 205 mA h g^{-1}, no capacity fading was observed after 70 cycles between 4.3 and 2.75 V at the 1 C rate. Differential scanning calorimetry (DSC) studies of the charged electrode at 4.3 V show a close relationship between particle size (BET surface area) and thermal stability of the electrode, namely, a larger particle size (smaller BET surface area) leads to a better thermal stability of the $LiNi_{0.74}Co_{0.26}O_2$ cathode.

Keywords: Lithium-ion battery; Particle size; Surface area; Thermal stability

1. Introduction

$LiNiO_2$ cathode material has received much attention for application in Li-ion batteries due to its higher specific capacity than $LiCoO_2$ and $LiMn_2O_4$ phases [1–5]. The specific capacity of $LiMn_2O_4$ and $LiCoO_2$ is about 120 and 160 mA h g^{-1}, respectively, while that of $LiNiO_2$ is about 208 mA h g^{-1} at a 4.3 V charge cut-off [1]. $LiNiO_2$ shows cycling-induced microcracks due to structural transformations of the hexagonal phases above 4.2 V; these cause rapid capacity fading on cycling [6]. When x is smaller than 0.3 in Li_xNiO_2, the lattice parameter c rapidly decreases to 13.5 Å from 14.4 Å, while the lattice parameter a remains almost constant. This corresponds to a 9% change in the volume of the structure which exceeds the elastic strain tolerance of the oxides including the cathode materials. Hence, such non-uniform volume changes along the c direction causes fracture in the $LiNiO_2$ particles. Similar behavior is also observed in the $LiCoO_2$ system [7].

In order to suppress such a structural transformation which causes capacity fading, $LiNi_{1-x}M_xO_2$ materials (M=transition metal) have been investigated [1,8–14]. The disadvantage of these materials, however, is that their thermal stability is inferior to that of $LiCoO_2$ and $LiMn_2O_4$ phases in spite of the higher specific capacity [1,15–17]. Dahn et al. [17] have shown that, at or above some critical temperature, Li_xNiO_2 is a significantly unstable compared to Li_xCoO_2 and $LiMn_2O_4$ and liberates oxygen as a result of decomposition into M_xO_y (M=Co or Mn) and O_2. The $LiNiO_2$ phase also shows a lower onset temperature of the exothermic peak at around 30–40°C. The amount of oxygen generated was estimated by thermal analyses using differential thermal analysis (DTA) or differential scanning calorimetry (DSC) measurements. The presence of oxygen gas as a result of decomposition of the charged cathode significantly affects the safety of the Li-ion cell. Abuse conditions, such as short-circuits and overcharge, accelerate the rate of heat generation exponentially, and cause thermal runaway. This can lead to catastrophic failure of the cell, including violent venting or rupture along with ignition of the components. To improve the thermal instability of Li_xNiO_2, Cho et al. [1] and Gao et al. [18] have studied the $LiNi_{1-y}Co_yO_2$ system. The results have shown that the increase in Co over Ni in $LiNi_{1-y}Co_yO_2$ leads to the improved thermal stability of $Li_xNi_{1-y}Co_yO_2$. Similar to this, partial substitution of Ni into Al in $LiNi_{1-y}Al_yO_2$ decreases the generation of O_2 from the charged cathode [19]. This effect is partially due to the decreased charge capacity of $LiNi_{1-y}Al_yO_2$ to that of $LiNiO_2$. The charge

* Corresponding author. Fax: +82-417-560-3789.
E-mail address: jpcho@samsung.co.kr (J. Cho).

0378-7753/01/$ – see front matter
PII: S0378-7753(00)00499-7

capacity of $LiNi_{0.75}Al_{0.25}O_2$ (at 4.5 V) decreases to 200 mA h g^{-1} from 250 mA h g^{-1} of $LiNiO_2$. The above studies deal with the effect of dopants in $LiNiO_2$, but not with the effect of the particle size (Brunauer, Emmett and Teller (BET) surface area) of the material. Therefore, in this study, we investigate the electrochemical and thermal properties of the $Li_xNi_{0.74}Co_{0.26}O_2$ material with different particle sizes, prepared from the reaction of co-precipitated $Ni_{0.74}Co_{0.26}(OH)_2$ and $LiOH{\cdot}H_2O$.

2. Experimental

Spherical $Ni_{0.74}Co_{0.26}(OH)_2$ powders (Fig. 1) were prepared, in a reactor, by co-precipitation of Ni nitrate and Co nitrate in a mixed solution of MH_4OH and NaOH. The co-precipitated powders were obtained at pH=10 and the pH condition was controlled by NaOH. The size of the particles (5, 13 and 25 μm) was controlled by the reaction time in the reactor; a longer reaction time led to a larger particle size. The powder morphologies of 13 and 25 μm-sized particles are different from that of 5 μm particles in that the particles consist of sub-micron-sized grains with a well-developed needle shape, as shown in Fig. 1. The $LiNi_{0.74}Co_{0.26}O_2$ compound was prepared by the reaction of co-precipitated $Ni_{0.74}Co_{0.26}(OH)_2$ and $LiOH{\cdot}H_2O$ with a mole ratio of 1:1.03 in a stream of dried air at 700°C for 15 h. An excess amount of Li was used for compensating the loss of Li during firing. The resultant powders exhibit spherical morphologies which are identical to that of the starting powder $Ni_{0.74}Co_{0.26}(OH)_2$, and the particles consist of rock-shaped grains (Fig. 2).

Coin-type test cells (size 2016) prepared in a helium-filled glove box contained a positive electrode (cathode), an Li metal negative electrode (anode), a microporous polyethylene separator, and an electrolyte consisting of a 1 M solution of $LiPF_6$ in a 1:1 (by volume) mixture of ethylene carbonate (EC) and dimethyl carbonate (DMC). Each test cathode contained approximately 25 mg of $LiNi_{0.74}Co_{0.26}O_2$. The test cells were aged at room temperature for 24 h after addition of the electrolyte before electrochemical testing. Cycling tests were carried out (charge cut-off voltage of 4.3 V at various charge and discharge rates of constant current) by means of a multi-channel Toyo Cycler with a current accuracy of better than 0.5%. Cycling tests were carried out initially by charging and discharging each cell at the 0.1 C (=18 mA h g^{-1}) rate for one cycle followed by three cycles at the 0.2 C rate, 10 cycles at the 0.5 C rate, and finally, at the 1 C rate for a total of 70 cycles. DSC samples of the cathode were prepared by charging the coin cells to 4.3 V at the 0.1 C rate, followed by holding them at the respective potential for 20 h. These cells were then dissembled in a glove box to remove the charged cathode which typically contained 30–35 wt.% electrolyte, 30 wt.% Al foil, 5 wt.% combined binder and carbon black, and 30–35 wt.% cathode material. A quantity of approximately 10 mg of the cathode was cut and hermetically sealed in an aluminum DSC sample pan. Only the cathode material

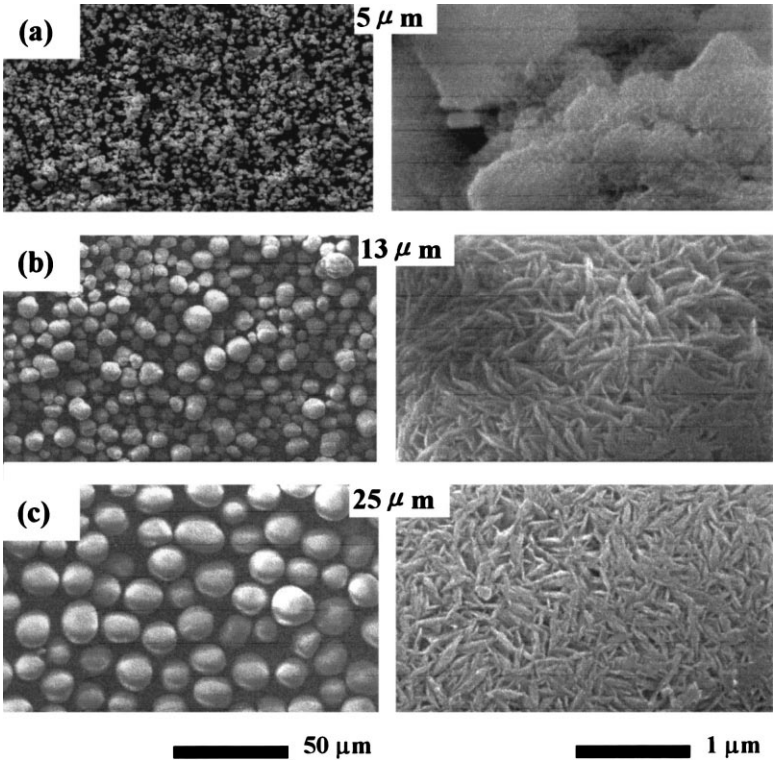

Fig. 1. SEM micrographs of co-precipitated $Ni_{0.74}Co_{0.26}(OH)_2$ with particle sizes of: (a) 5 μm, (b) 13 μm, (c) 25 μm.

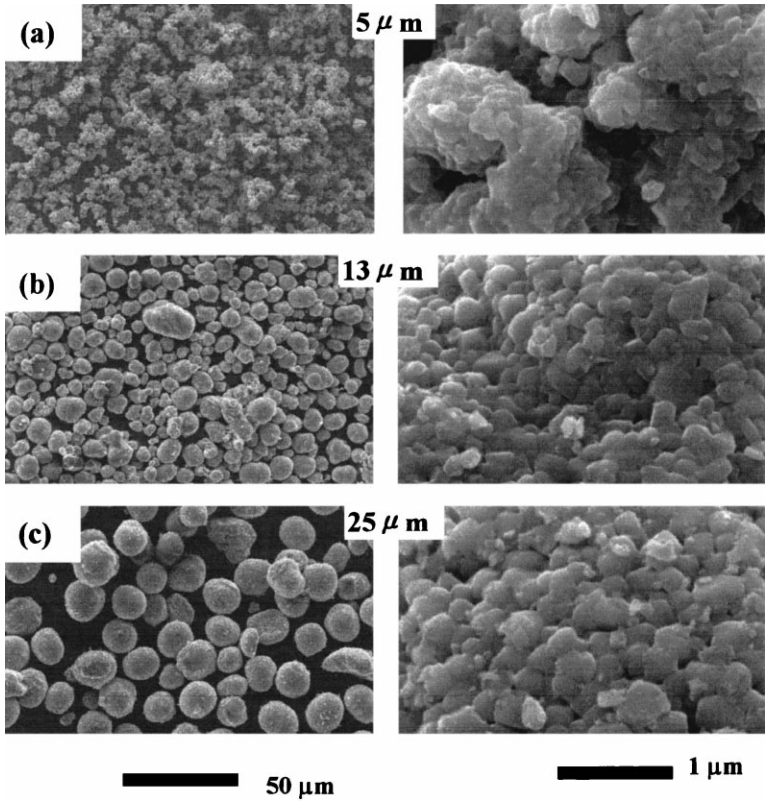

Fig. 2. SEM micrographs of $LiNi_{0.74}Co_{0.26}O_2$ with particle sizes of: (a) 5 μm, (b) 13 μm, (c) 25 μm. The material was prepared via reaction of $Ni_{0.74}Co_{0.26}(OH)_2$ with $LiOH{\cdot}H_2O$ at 700°C for 15 h.

was used for the calculation of specific heat flow, with a heating rate of 3°C min^{-1}.

3. Results and discussion

The X-ray diffraction pattern (Fig. 3) of $LiNi_{0.74}Co_{0.26}O_2$ shows that it is isostructural with α-$NaFeO_2$ and has a space group R-3m in which Li and Co/Ni ions occupy 3*a* and 3*b* sites, respectively, on an alternate (1 1 1) plane of the rock salt structure, while the oxygen ions form a close-packed face centered cubic (fcc) structure [20]. The lattice parameters *a* and *c* of $LiNi_{0.74}Co_{0.26}O_2$ are 2.863 and 14.168 Å, respectively. As shown in Fig. 4, $LiNi_{0.74}Co_{0.26}O_2$ shows the highest capacity except for y=0 and y=0.1 in the series of $LiNi_{1-y}Co_yO_2$. The cycle-life of the material improves with increasing Co addition in $LiNi_{1-y}Co_yO_2$ [1,10,12].

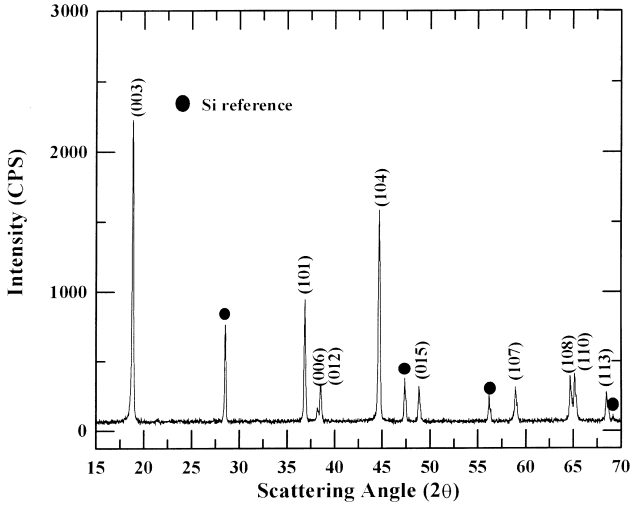

Fig. 3. XRD pattern for $LiNi_{0.74}Co_{0.26}O_2$ powders.

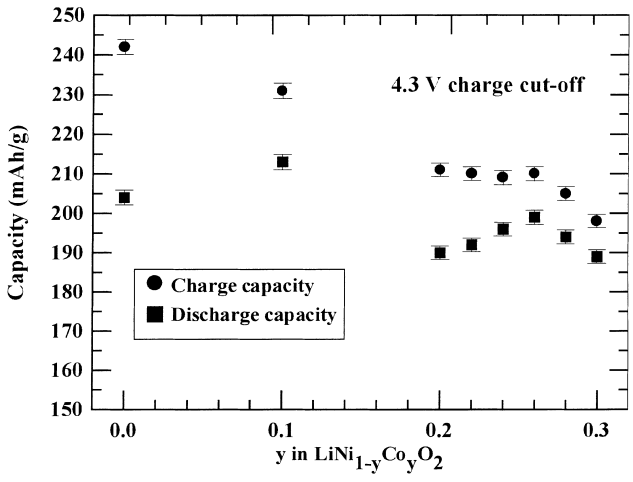

Fig. 4. Plot of capacity variation for $LiNi_{1-y}Co_yO_2$ as a function of *y*.

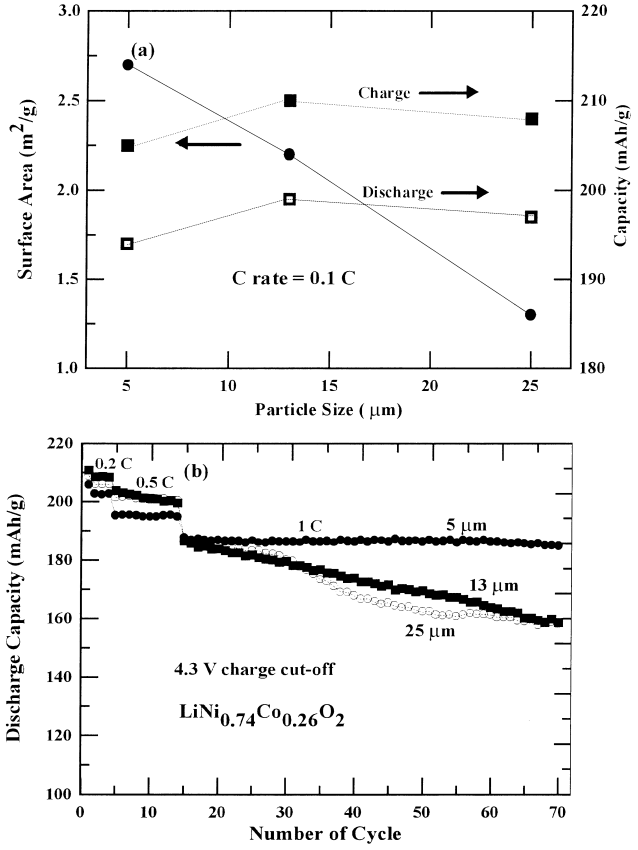

Fig. 5. (a) Charge and discharge capacities, and BET surface areas of $LiNi_{0.74}Co_{0.26}O_2$ with particle sizes of 5, 13 and 25 μm. (b) Capacity retention of $LiNi_{0.74}Co_{0.26}O_2$ with particle sizes of 5, 13 and 25 μm against the number of cycles in coin-type half cells of $Li/LiNi_{0.74}Co_{0.26}O_2$. The cells were initially cycled once at charge and discharge rates of 0.1 C, followed by three cycles at the 0.2 C rate, 10 cycles at the 0.5 C rate, and finally, at the 1 C rate for a total of 70 cycles.

The highest value of the discharge capacity of the material with a particle size of 13 μm is 210 mA h g^{-1}, but those with particle sizes of 5 and 25 μm show discharge capacity values of 205 and 208 mA h g^{-1}, respectively, between 4.3 and 2.75 V at the 0.1 C rate (=18 mA g^{-1}). The BET surface area of the material, as expected, decreases proportionally with increase in the particle size, and thus, the material with 25 μm-sized particles displays the lowest value of BET area of 1.3 m^2 g^{-1}, as shown in Fig. 5a. The capacity retention of $LiNi_{0.74}Co_{0.26}O_2$ with 5, 13 and 25 μm-sized particles is determined by increasing, in a stepwise manner, the charge rate from 0.1 to 1 C (Fig. 5b). The $LiNi_{0.74}Co_{0.26}O_2$ electrode with 5 μm-sized particles exhibits higher capacity retention at the 1 C rate and negligible capacity loss after 70 cycles between 4.2 and 2.75 V at the 1 C rate (=180 mA g^{-1}) as compared to those of 13 and 25 μm-sized particles. This difference may be due to the reduced polarization at the surfaces of particles, which is due to the increased BET surface area. Still, the capacity retention of the material having particle sizes of 13 and 25 μm is 50% higher than that of $LiNiO_2$. This difference can be explained by examining the cyclic voltammograms of $LiNiO_2$ and

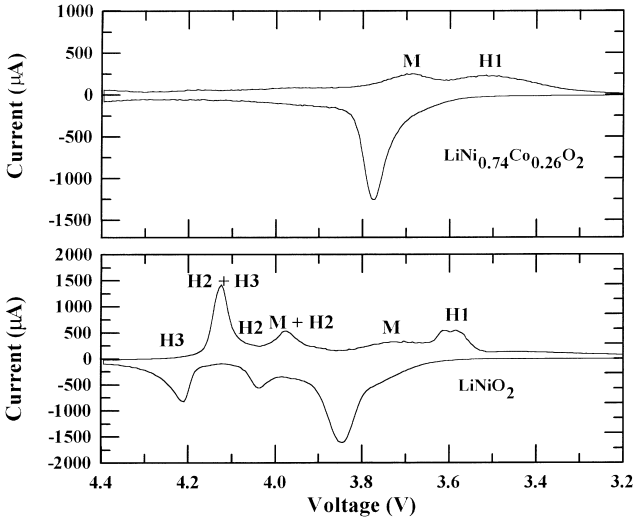

Fig. 6. Cyclic voltammograms of: (a) $LiNi_{0.74}Co_{0.26}O_2$ and (b) $LiNiO_2$. Scan rate=0.02 mV s^{-1}.

$LiNi_{0.74}Co_{0.26}O_2$ (Fig. 6). The $LiNiO_2$ phase shows two electrochemical couples, M+H2 and H2+H3. The M+H2 peak signifies a transition between a monoclinic phase (M) and a hexagonal phase (H2), and H2+H3 represents a transition between a hexagonal phase (H2) and another hexagonal phase (H3) [20]. Compared to the $LiNiO_2$ compositional redox couples, H2+H3 and M and H2 in $LiNi_{0.74}Co_{0.26}O_2$ almost disappear. It has been reported [6] that the rapid volume shrinkage during the structural transformation from H2 to H3 mostly influences the capacity fading of the material [6]. Hence, good reversibility of $LiNi_{0.74}Co_{0.26}O_2$ is believed to be due to suppression of the H2+H3 transition.

Thermal stability of the $LiNi_{0.74}Co_{0.26}O_2$ electrode charged at 4.3 V was tested by performing DSC experiment, as shown in Fig. 7. The exothermic peak area, corresponding to the amount of oxygen generated from the decomposition of the electrode material, increases with rapid increase in the particle size (i.e. increase in the BET surface area). Hence, the electrode with 5 μm-sized particles shows the highest

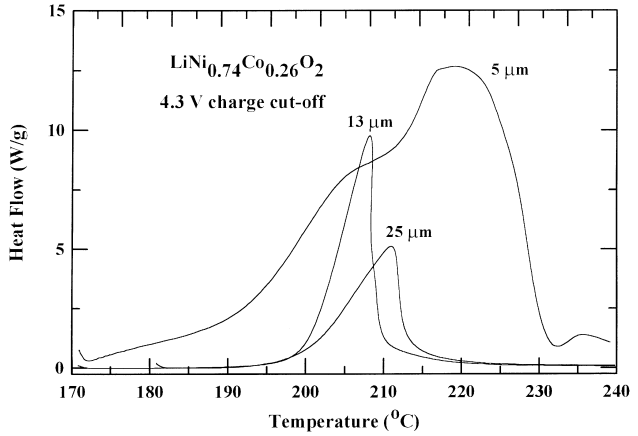

Fig. 7. DSC scans of charged $LiNi_{0.74}Co_{0.26}O_2$ to 4.3 V with different particle sizes of 5, 13 and 25 μm. Heating rate=3°C min^{-1}.

amount of heat liberated by the decomposition, compared to electrodes with 13 and 25 μm-sized particles. It is important to note the improved onset temperature (∼200°C) of the exothermic peaks of the 13 and 25 μm-sized particles compared to that of the 5 μm-sized particles. The high exothermic peak with a lower onset temperature of the material with 5 μm-sized particles is because higher BET surface area provides more reaction sites with the electrolyte.

4. Conclusions

Spherical $LiNi_{0.74}Co_{0.26}O_2$ powders with particle sizes of 5, 13 and 25 μm have been prepared from the reaction of co-precipitated $Ni_{0.74}Co_{0.26}(OH)_2$ and $LiOH{\cdot}H_2O$ at 700°C. Even though the material with 5 μm-sized particles shows the highest capacity retention at the 1 C rate, its thermal stability is deteriorated by the high BET surface area. Overall, $LiNi_{0.74}Co_{0.26}O_2$ with particle sizes of either 13 or 25 μm may be the best candidate as a cathode material for Li-ion cells.

References

[1] J. Cho, H. Jung, Y. Park, G. Kim, H. Lim, J. Electrochem. Soc. 147 (2000) 15.
[2] R. Kanno, H. Kubo, Y. Kawamoto, T. Kamiyama, F. Izumi, Y. Takeda, M. Takano, J. Solid State Chem. 110 (1994) 216.
[3] J. Morales, C. Perez-Vicente, J.L. Tirado, Mater. Res. Bull. 25 (1990) 623.
[4] S. Yamada, M. Fujiwara, M. Kanda, J. Power Sources 54 (1995) 209.
[5] R.V. Moshtev, P. Zlatilova, V. Manev, A. Sato, J. Power Sources 54 (1995) 329.
[6] K. Dokko, M. Nishizawa, S. Horikoshi, T. Itoh, M. Mohamed, I. Uchida, Electrochem. Solid State Lett. 3 (1999) 3.
[7] H. Wang, Y. Jang, B. Huang, D.R. Sadoway, Y. Chiang, J. Electrochem. Soc. 146 (1999) 473.
[8] J. Cho, G. Kim, H. Lim, J. Electrochem. Soc. 146 (1999) 3571.
[9] H. Watanabe, T. Sunagawa, H. Fujimoto, N. Nishida, T. Nohma, Sanyo Tech. Rev. 30 (1998) 84.
[10] J. Cho, G. Kim, Y. Park, H. Lim, in: Proceedings of the 15th International Seminar on Primary and Secondary Batteries, Fort Lauderdale, FL, 2–5 March 1999.
[11] C. Delmas, I. Saadoune, A. Rougier, J. Power Sources 43 (1993) 595.
[12] T. Ohzuku, A. Ueda, M. Nagayama, J. Electrochem. Soc. 140 (1993) 1862.
[13] J.R. Dahn, E.W. Fuller, M. Obrovac, U. von Sacken, Solid State Ionics 69 (1992) 12.
[14] W. Li, J. Currie, J. Electrochem. Soc. 144 (1997) 2773.
[15] Z. Zhang, D. Fouchard, J.R. Rea, J. Power Sources 70 (1998) 16.
[16] J. Cho, G. Kim, Electrochem. Solid State Lett. 2 (1999) 253.
[17] J.R. Dahn, E.W. Fuller, M. Obrovac, U. von Sacken, Solid State Ionics 109 (1994) 265.
[18] Y. Gao, M.V. Yakovleva, W.B. Ebner, Electrochem. Solid State Lett. 1 (1998) 117.
[19] T. Ohzuku, T. Yanagawa, M. Kouguchi, A. Ueda, J. Power Sources 68 (1997) 131.
[20] W. Li, J.N. Reimers, J.R. Dahn, Solid State Ionics 67 (1993) 123.